Reprinted from June 1976, Vol. 98, Journal of Fluids Engineering

The Dynamic Transfer Function for a Cavitating Inducer

C. BRENNEN

A. J. ACOSTA

Mem. ASME

California Institute of Technology, Pasadena, Calif.

Knowledge of the dynamic performance of pumps is essential for the prediction of transient behavior and instabilities in hydraulic systems; the necessary information is in the form of a transfer function which relates the instantaneous or fluctuating pressure and mass flow rate at inlet to the same quantities in the discharge from the pump. The presence of cavitation within the pump can have a major effect on this transfer function since dynamical changes in the volume of cavitation contribute to the difference in the instantaneous inlet and discharge mass flow rates. The present paper utilizes results from free streamline cascade theory to evaluate the elements in the transfer function for a cavitating inducer and shows that the numerical results are consistent with the characteristics observed in some dynamic tests on rocket engine turbopumps.

Introduction

The development in recent times of high speed and high performance pumps for liquids and their inclusion in increasingly complex hydraulic systems has created a need for improvement in our understanding of these flows. Demands of space and economy almost invariably lead to pump (or turbine) designs which operate either with cavitation or sufficiently close to that point, so that significant perturbations lead to cavitation. Sometimes the demands of pump size or mass are exceedingly stringent as in rocket engines (or propulsion devices of other high performance vehicles) so that the pumps operate with extensive cavitation at the inlet. In other situations high temperatures and velocities plus the need to economize on highly expensive equipment draw the designer ever closer if not beyond the point of cavitation inception; such appears to be the case in the boiler feed and coolant systems not only of conventional but also of nuclear generating plants. Another situation occurs in systems such as those associated with geothermal generating plants where flashing of two phases can lead to cavitation-like phenomena in the pumps and turbines. With regard to turbines one should remember that cavitation phenomena similar to those at pump inlet also occur on the outlet side of turbines where there exists an analogous set of conditions; though we will speak here only of pumps the complementary problem in turbines should be borne in mind.

Major problems remain in connection with the steady-stat operation of such cavitating pumps and turbines. The prediction of the advent of cavitation, the form it takes, its effect upon performance and the material damage it can cause are still subjects of intensive research. But it is rapidly becoming apparent that a whole new set of technological problems are arising which involve the dynamic rather than the steady state operation of such turbomachines. Formerly it was sufficient for the designer to analyze the steady-state operation of a hydraulic system. With the increasing complexity dynamic and stability analyses are now desirable for pumping systems and are required for hydropower installations [1, 2].[1] Transient problems also occur in boiler feed systems [3, 4] and the resonances of fully wetted hydraulic systems have received recent attention [5]. When a second phase makes its appearance analysis of these systems becomes considerably more complex. The fluid may then be considered as a mixture (e.g., [6]) or the liquid column may be assumed to divide into distinct parts separated by vapor [7, 8].

These studies have concentrated attention almost entirely on the unsteady flow within the pipeline components of hydraulic systems even though it is known that any associated fluid machine participates in the unsteady motion. The first step in providing a fuller knowledge of the complete performance characteristics of a pump or turbine was probably taken by Knapp [9]. The now well-known circle diagram provides the steady-state behavior for all combinations of flow (quantity and direction) and rotative speed (including sense). The unsteady tests carried out by Knapp to verify the use of the complete characteristic

Contributed by the Fluids Engineering Division of THE AMERICAN SOCIETY OF MECHANICAL ENGINEERS and presented at the Winter Annual Meeting, Houston, Texas, November 30-December 4, 1975. Manuscript received at ASME Headquarters August 15, 1975. Paper No. 75-WA/FE-16.

[1] Numbers in brackets designate References at end of paper.

were done at such a low frequency that the steady behavior was entirely sufficient. In modern applications however the frequency of the unsteady-perturbations may get quite high. Although the dynamic effect associated with any disturbance frequency can only be evaluated properly as a dimensionless reduced frequency, it seems reasonable that there should be a modification of the basic steady-state characteristics for higher frequencies. Yet one of the stumbling blocks for the dynamic analysis of these modern applications is often the almost total lack of knowledge of the dynamic behavior of a pump or turbine, particularly when there is cavitation present It may be expected that a full understanding of these relations would at the very least be exceedingly complex. Fortunately for many if not most hydraulic system response analyses it is sufficient to deal with small departures from some average state of operation. These small departures are then usually assumed to be related by linear equations. Thus it becomes possible to relate fluctuating inlet quantities to corresponding outlet ones by means of linear equations of the form (for constant rotative speed)

$$\begin{Bmatrix} \tilde{p}_2 - \tilde{p}_1 \\ \tilde{m}_2 - \tilde{m}_1 \end{Bmatrix} = \begin{bmatrix} Z_{11} & Z_{12} \\ Z_{21} & Z_{22} \end{bmatrix} \begin{Bmatrix} \tilde{p}_1 \\ \tilde{m}_1 \end{Bmatrix}. \quad (1)$$

In this equation $\tilde{p}_1$, $\tilde{m}_1$ refer to the fluctuating inlet pressure and mass flow rate and $\tilde{p}_2$, $\tilde{m}_2$ to the corresponding discharge quantities. The matrix $[Z]$ is called the *transfer matrix*. Generally the coefficients may be expected to depend on frequency, the operating point and degree of cavitation. For very low frequencies equation (1) should reduce to the usual steady state operating characteristics of a flow machine. In this limit we can identify Z_{11} as the slope of the pressure-rise versus inlet pressure curve at constant speed; this is the familiar cavitation performance curve. Furthermore, Z_{12} can then be interpreted as the slope of the pressure rise—mass flow curve; that is, it is just the slope of the "H-Q" curve at that particular operating point. Cavitation plays a major role in this transfer function since oscillation in the volume of cavitation is often the only significant source for the difference between the instantaneous inlet and discharge mass flows. Indeed if liquid compressibility and structural compliance were negligible Z_{21} and Z_{22} would be zero in the absence of cavitation and the dynamic characteristics would then be much simpler. In the presence of cavitation we are faced with the problem of evaluating the four complex or eight real elements of $[Z]$ (the variables $\tilde{p}_1$, $\tilde{p}_2$, $\tilde{m}_1$ and $\tilde{m}_2$ being complex in order to incorporate both their amplitude and their phase relationships) as functions not only of frequency, Ω, but also of the steady-state operating conditions, including the cavitation number σ, which characterizes the extent of cavitation in the pump. Furthermore, it should be noted that $[Z]$ as defined in equation (1) is probably the minimum information required; the size of the matrix could be further increased by the incorporation of other independent fluctuating quantities such as rotational speed of the pump impeller. In some turbomachinery applications such fluctuations in the rotational speed may be a relatively passive effect, that is to say a response to the fluctuating loads on the impeller blades. In other situations such as in rocket engines the pump may be driven by a turbine powered by fluid bled from the throughflow so that additional dynamic interactions are present. In either case the matrix elements which characterize this situation would clearly include properties of the mechanical drive train and its prime mover. Some considerations of the effects of rotational speed fluctuations will be included in Appendix I.

The purpose of the present work is to outline a procedure to evaluate the elements of the transfer matrix for *low frequencies*. This may be regarded as a first step to extend the pump characteristics into the region of unsteady operation. The basic means of analysis for this work is quasi-steady free-streamline cascade theory. In what follows the relation between this type of cavitation and what is observed is compared for some representative pump impellers. The terms of the transfer function can then be evaluated and compared in the limit of low frequency with current lumped parameter models of cavitating pumps.

Nomenclature

a = nondimensional cross-sectional cavity area, A^*/h^2
A^* = cross-sectional cavity area
A_i = inducer inlet area
A, B = complex constants
C, C_B, C_2 = dimensional compliances
$d(r)$ = ratio of blade thickness to normal blade spacing at radius, r
G = pump gain
$h(r)$ = leading edge spacing at radius, r
H = leading edge spacing at tip, $h(R)$
i = spacewise imaginery unit
j = timewise imaginery unit
K_L = local nondimensional compliance
K_B = overall nondimensional compliance
L = fluid inertance
$\tilde{m}$ = nondimensional oscillatory mass flow rate, $\tilde{m}^*/\rho A_i U_T$
$\tilde{m}^*$ = oscillatory mass flow rate
M_L = local mass flow gain factor (nondimensional)
M_B = overall mass flow gain factor (nondimensional)
M_B^* = a dimensional mass flow gain factor
N = number of inducer blades
$\tilde{N}$ = fluctuating rotational speed of inducer
N_L = local rotational influence factor
N_B = overall rotational influence factor
p^* = pressure
p_C = cavity pressure
$\tilde{p}^*$ = oscillatory pressure
$\tilde{p}$ = nondimensional oscillatory pressure
r = radial coordinate in the inducer
R = radius of inducer tip
R_H = radius of inducer hub
R_1, R_2 = fluid resistances
R_P = pump resistance
R_D = discharge resistance
u, v = fluid velocities in x, y directions
U_F = axial fluid velocity at inducer inlet
$U_B(r)$ = blade velocity at radius, r
U_T = inducer tip speed, $U_B(R)$
$U_1(r)$ = fluid velocity relative to blades at radius, r
V = total cavity volume
w = complex velocity, $u - iv$
x, y = cartesian coordinates in cascade plane
z = $x + iy$
Z = transfer matrix and its elements
$\alpha(r)$ = angle of attack at radius, r
$\beta(r)$ = blade angle at radius, r
ζ = complex variable in transformed plane
ρ = liquid density
$\sigma_L(r)$ = local cavitation number at radius, r
σ_T = overall or tip cavitation number, $\sigma_L(R)$
φ = flow coefficient, U_F/U_T
ω = nondimensional fluctuation frequency, $\Omega H/U_T$
Ω = fluctuation frequency

Subscripts

1 = conditions at inducer inlet
2 = conditions at inducer discharge

A new factor is seen to be required which appears to remove much of the discrepancy between theoretically derived transfer function elements and those deduced from flight and field tests.

Background

Before proceeding it is worth describing a specific example of a pump application problem in which knowledge of the transfer function is essential. Virtually all liquid-propelled rockets are susceptible to an instability which involves a closed loop interaction between the longitudinal structural modes of vibration of the vehicle and the dynamics of the propulsion system [10, 11] This so-called "POGO" instability is an extreme hazard since it can lead to excessive accelerations of the payload, stresses on the structure and possible premature shutdown. Simplistically described, the instability involves longitudinal structural vibrations which lead to pressure fluctuations in the fuel and oxidizer tanks, and to pressure and mass flow oscillations in the feedlines. The cavitating propellant pumps thus experience fluctuating inlet conditions and as a result the engines can produce an oscillating thrust which can lead to further amplification of the longitudinal structural vibration. Most of the essential elements in this system are well understood and quantifiable dynamically with the notable and important exception of the turbopumps. We cite this particular example because it is one of the few situations in which detailed attempts have been made to analyze and measure the dynamic characteristics of cavitating turbomachines.

Quantitative details are not readily avaiable for commercial and utility applications often for proprietary and legal reasons (hence the paucity of reference here). Informal reports of disastrous resonances involving cavitation in the suction lines and pumps of boiler feed systems do persist however. Sometimes such problems are manifest during transient operation [3, 4]: in other situations cavitation-induced resonances may occur. The latter have been the subject of recent studies by Sack Nottage [12] and Natanzon, et al. [13] which are in the same spirit as the present paper.

Transfer Matrix, Frequency Dependence

Fortunately in many practical situations the frequencies, Ω, are sufficiently small to suggest reasonable validity for solution of the matrix elements in series with ascending powers of Ω. We have previously indicated [14] that the reduced frequencies involved in the POGO instability are often small enough for such a procedure. Thus, in the present paper we shall focus attention on the first nonzero term in the series for each element in $[Z]$. The zeroth order or frequency independent terms in Z_{11} and Z_{12} should as previously discussed then be given by the steady-state operating characteristics of the pump (see, for example, Wagner [15]); the former by the slope of the steady state curve of pressure rise against inlet pressure and the latter by the slope of the pressure rise versus flow rate for a given inlet pressure. Therefore we shall concentrate here on the terms Z_{21} and Z_{22} which must begin with terms linear in frequency since the mass flow difference is zero in steady-state operation. However, we shall see that values for Z_{21} and Z_{22} can be deduced from knowledge of a series of quasi-static or steady cavitating flows through an inducer. On the other hand, in order to obtain the second terms in each of the elements it is necessary to solve the difficult fundamental problem of truly unsteady flow in a cavitating pump. Though the latter task is becoming feasible for an axial inducer through the work of Kim and Acosta [16] and Furuya [17], the present paper will concentrate on the evaluation of the first terms in Z_{21} and Z_{22}.

These elements relate the instantaneous difference between the inlet and outlet mass flows to the inlet fluctuating conditions

$$Z_{21} = \left(\frac{\tilde{m}_2 - \tilde{m}_1}{\tilde{p}_1} \right)_{\tilde{m}_1 = 0} ; \quad Z_{22} = \left(\frac{\tilde{m}_2 - \tilde{m}_1}{\tilde{m}_1} \right)_{\tilde{p}_1 = 0} \tag{2}$$

where $\tilde{p}_1$, $\tilde{p}_2$, $\tilde{m}_1$, $\tilde{m}_2$ denote dimensionless fluctuating pressures and mass flows at inlet and discharge (for definition see equations [8]). In dynamic operation the mass flow difference is, of course, caused by the growth or shrinkage of the total volume of cavitation within the pump. Thus Z_{21} and Z_{22} are directly linked with cavitation and the purpose here will be to develop and construct this relationship.

Up to the present time dynamicists concerned, for example, with analysis of the POGO instability (e.g., Rubin [11], Rubin, Wagner and Payne [18]) have been required to make some dynamic model of a cavitating turbopump and have thus resorted to some rather arbitrary assumptions. Until recently it was conventional, for example, to assume that all of the cavitation could be lumped into a single bubble at the inlet side of the pump and to assume that this bubble had a simple spring-constant response to the fluctuating pressure at inlet. This response was termed the cavitation compliance of the inducer and is related to some value for Z_{21}. More recently data on this cavitation compliance has been collected by Ghahremani and Rubin [19], Brennen and Acosta [14] and Brennen [20] with the intent of relating that quantity to the extent and type of cavitation expected.

Further, it seems to have been universally assumed for lack of any other knowledge that Z_{22} was identically zero. A particular purpose of this paper is to demonstrate that according to the present calculations for typical inducers Z_{22} is far from zero and may indeed represent a major dynamic effect.

Since cavitation in an inducer can take a number of forms (see Brennen [20] for example) it has proved convenient to separately investigate the dynamics of each form. The compliance of fully developed blade cavities was investigated by Brennen and Acosta [14] and that of bubble cavitation by Brennen [20]. In the latter it was shown that bubble cavitation is capable of contributing substantially to the compliance in the

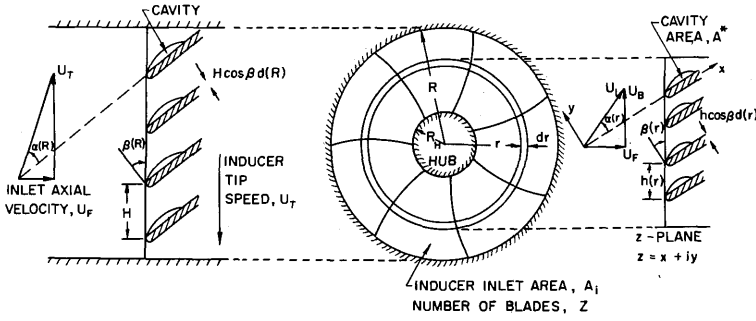

Fig. 1 Inducer inlet with nomenclature

absence of blade cavitation. But when blade cavitation occurs, the pressure in the fluid exterior to the blade cavity is generally above the vapor pressure and hence there is little bubble cavitation, except in the tip clearance and backflow regions. Neglecting these other features, it would seem plausible to argue that when cavitation is sufficiently extensive for blade cavities to be formed the latter would contribute a major part of the compliance. Yet the theoretically calculated blade cavitation compliances of Brennen and Acosta [14] are generally much smaller than those deduced from experimental observation by Vaage, Fidler and Zehnle [21]. The present paper addresses itself to this discrepancy and demonstrates that its cause probably lies in the hypothetical dynamic model which is employed in order to deduce the compliance from the experimental measurements. It is demonstrated that for most of the cavitation number range, the factor Z_{22} is as important as Z_{21} in determining the dynamic effect of the cavitation and that the calculated values of Z_{22} are in fair agreement with the dynamic effect deduced from tests.

Finally we should mention that Kolesnikov and Kinelev [32] have presented a theoretical analysis of the dynamic behavior of cavitating pumps by considering the entire flow between blades to consist of a liquid/bubble mixture; they proceed to evaluate the dynamic effects associated with this mixture and the much reduced sonic velocity they ascribe to it. No quantitative data is presented and apart from the overly simplistic view of cavitation and the basic mixture assumptions, other empirical relations assumed make it difficult to assess the value of their analysis.

Axial Inducer Cascade Solutions

An axial inducer designed to operate with cavitation is a common feature of high performance pumps and it is to this component, the principle source of cavitation in a pump that present effort is directed. The flow in an inducer is exceedingly complex (noncavitating inducer flows have been extensively treated recently by Lakshminarayana [27]) and it is necessary to make rather crude assumptions in order to construct even approximate flow solutions. Frequently it is assumed that the radial velocity components in the inducer can be neglected so that each radial station can then be unrolled into a cascade as indicated in Fig. 1. Free streamline potential flow models of these annular cascades have been employed extensively in the past to study steady cavitating flow in turbomachines. Most of the flow solutions have been based on a linearized approach, (Cohen and Sutherland [22], Acosta and Hollander [23], Acosta [24], Wade [25]), although Stripling and Acosta [26] have also considered the more exact nonlinear cavitating cascade problem. Unfortunately all of these methods are significantly deficient in that they assume infinitely thin blades and thus neglect the often critical effects of blade thickness. Brennen and Acosta [14] attempted to rectify this in presenting a simple linearized solution which includes finite blade thickness. The cascade in the $z = x + iy$-plane is first conformally mapped into the ζ-plane of Fig. 2 by

$$2\pi(z/h) = e^{-i\beta}\ln(1 - \zeta/\zeta_1) + e^{i\beta}\ln(1 - \zeta/\bar{\zeta}_1).$$

The linearized free streamline solution of this problem for infinitely thin blades was first given by Acosta and Hollander [23] and consists of the first three terms on the right hand side of equation (3) for the complex velocity, $w = u - iv$ (u, v are velocity components in x, y directions). Brennen and Acosta [14] added the fourth term and showed that this represented a simple solution for the case of blades with the ultimate thickness $dh \cos\beta$

$$\frac{w(\zeta)}{U_1} = B\left(\frac{\zeta}{\zeta - l}\right)^{1/2} - A\left(\frac{\zeta - l}{\zeta}\right)^{1/2} + (1 + \sigma_L)^{1/2} - \frac{id\cos\beta}{\zeta} \quad (3)$$

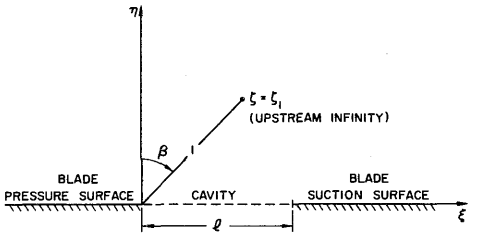

Fig. 2 Transformed ζ-plane for linearized solution of flow in cavitating cascade

The cavitation number, σ_L, is defined in the conventional way as $(p_1^* - p_C)/{}^1/_2\rho U_1^2$ where p_1^*, p_C are the upstream and cavity pressures, U_1 is the inlet fluid velocity relative to the blades and ρ the liquid density. The complex constants A, B are then obtained from the conditions at upstream and downstream infinity and a continuity condition (which involves d). Finally the solution (3) and the cavitation number, σ_L, can be written in terms, of d, α, β, h, U_1 and a convenient parameter, l, representing the length of the cavity in the transformed plane. Ordinates describing the shape of the foil profile and the cavity profile are then obtained and integration leads to a cavity area, A^*. or volume per unit depth of the plane flow. The dimensionless volume $a = A^*/h^2$ is then a function of the values of α, β, d and σ_L relevant to the particular cascade under consideration. Note that $\beta(r)$, $d(r)$ are fixed geometric functions of radial position, r, but that $\alpha(r)$ will vary with the flow coefficient, φ defined as U_F/U_T (where the fluid velocity, U_F, is assumed independent of r) according to

$$\alpha(r) = \frac{\pi}{2} - \beta(r) - \tan^{-1}\frac{R\varphi}{r} \quad (4)$$

where R is the radius of the inducer tip (velocity U_T). Furthermore the local value of σ_L will differ from the overall or tip cavitation number for the inducer, σ_T as given by the relation

$$\sigma_T = (p_1^* - p_C)/\frac{1}{2}\rho(U_T^2 + U_F^2) \quad (5)$$

where p_1^* is the inlet pressure. However, since U_F is usually small compared with U_T it follows that

$$\sigma_L(r) \approx R^2\sigma_T/r^2 \quad (6)$$

and hence the radial function $\sigma_L(r)$ is readily determined The total volume of cavity in the inducer, V, which is a function of the inducer operating conditions, φ, σ_T, can then be written as

$$V(\varphi, \sigma_T) = \int_{R_H}^{R} a(r, \sigma_L, \varphi) \times (h(r))^2 \times N dr \quad (7)$$

where N is the number of blades ($h(r) = 2\pi r/N$) and R_H is the radius of the hub The basic quantities a, $\partial a/\partial\sigma_L$ and $\partial a/\partial\alpha$ required in the following analysis (as functions of α, β, d, σ_L) were computed in a subroutine by methods similar to those used previously [14].

Quasistatic Analyses; Cavitation Compliance

We shall now relate the instantaneous mass flow rate difference $(\tilde{m}_1 - \tilde{m}_2)$ to the rate of change of the cavity volume V with the objective of evaluating Z_{21} and Z_{22} from equation (7). It will become clear that the most convenient manner in which to nondimensionalize the fluctuating pressures and mass flow rates and their frequency, Ω, is as follows:

$$\tilde{p} = \frac{\tilde{p}^*}{\frac{1}{2}\rho U_T^2} \; ; \; \tilde{m} = \frac{\tilde{m}}{\rho A_i U_T} \; ; \; \omega = \frac{\Omega H}{U_T} \quad (8)$$

where stars denote the corresponding dimensional quantities, A_i, is the inducer inlet area and ω is the reduced frequency.

Let us consider first the term Z_{21}; since this parameter is obtained with $\tilde{m}_1 = 0$ it follows that only σ_T, σ_L and not φ or α vary throughout a cycle of the fluctuations. The resulting cyclic change in the volume of the cavity is thus caused by fluctuations in the cavitation number alone. Thus following a quasistatic approach we may connect the cavity volume variation with the mass flow rate difference through the relation

$$Z_{21} = \frac{U_T}{2A_i}\left(\frac{\Delta(\tilde{m}_1{}^* - \tilde{m}_2{}^*)}{\Delta\tilde{p}_1{}^*}\right)_{\varphi=\text{const}} = \frac{j\Omega\rho U_T}{2A_i}\left(\frac{\partial V}{\partial p_1}\right)_{\varphi=\text{const}} \quad (9)$$

where j is the imaginary index. Then substituting for V from equation (7), taking the derivative inside the integral and making use of the approximate relation $\partial/\partial p_1 \equiv (r^2U_T{}^2/R^2)\partial/\partial\sigma_L$ the resulting expression for Z_{21} is most conveniently written as

$$Z_{21} = -j\omega K_B \quad (10)$$

where K_B is termed the *dimensionless* cavitation compliance of the pump and is given by

$$K_B(\varphi, \sigma_T) = \frac{2}{[1 - (R_H/R)^2]}\int_{RH/R}^{1} K_L(\varphi, \sigma_T, r/R)d(r/R) \quad (11)$$

where K_L is a local compliance being given by

$$K_L(\varphi, \sigma_T, r/R) = -\frac{\partial a}{\partial\sigma_L}. \quad (12)$$

Values of K_L are immediately available from the cascade solution once α, β, d and σ_L have been determined. Note that the choice of non-dimensional variables in equation (8) has resulted in the most convenient expressions for Z_{21}, K_B and K_L. Also note that the definition (11) has been arranged, so that if K_L increases linearly with r within the inducer, then the value of K_B is equal to the value of the local compliance K_L at the tip; frequently this is not a bad first approximation. Finally, it should be noted that the dimensionless compliance, K_B, is closely related through the expression $K_B = C_BU_T{}^2/2HA_i$ to the *dimensional* cavitation compliance, C_B, used by Ghahremani and Rubin [19], and others in connection with rocket turbopumps.

The above method for calculating a pump compliance, K_B, is essentially that employed previously by Brennen and Acosta [14]. The resulting theoretical values of K_B were found to be between three and ten times smaller than values derived from experiments on the F1, H1 and J2 Saturn engine turbopumps. As shown in the next section this is due to neglect of the term Z_{22} which we call the Mass Flow Gain Factor.

Mass Flow Gain Factor

Methods analogous to those of the previous section allow calculation of Z_{22} as well as Z_{21} (or K_B). By definition the compliance, K_B arises from the response of the cavity volume to fluctuations in the inlet pressure (or more specifically the cavitation number) while the inlet flow rate or flow coefficient remains constant. On the other hand, the quantity Z_{22} results from variations in the cavity volume because of fluctuations in the flow coefficient or angle of attack due to fluctuating inlet flow rate while the inlet pressure remains constant. Thus the evaluation of Z_{22} proceeds along lines similar to that of the last section except that the inlet pressure is maintained constant while the inlet flow rate varies. It follows from the definition (2) that

$$Z_{22} = \left(\frac{\Delta(\tilde{m}_1{}^* - \tilde{m}_2{}^*)}{\Delta\tilde{m}_{1\pm}{}^*}\right)_{\tilde{p}1^*=0} = j\frac{\Omega}{A_i}\left(\frac{\partial V}{\partial U_F}\right)_{\tilde{p}1^*=0}. \quad (13)$$

By analogy with the compliance derivation it is clear that we should define a dimensionless quantity, M_B, which we will term the mass flow gain factor (cf., equation (10))

$$Z_{22} = -j\omega M_B. \quad (14)$$

Substituting into equation (13) for V from the relation (7) one obtains

$$M_B(\varphi, \sigma_T) = \frac{2}{[1 - (R_H/R)^2]}\int_{RH/R}^{1} M_L(\varphi, \sigma_T, r/R)\left(\frac{r}{R}\right) d\left(\frac{r}{R}\right) \quad (15)$$

in which the local mass flow gain factor, M_L, defined in equation (15) is given by

$$M_L(\varphi, \sigma_T, r/R) = U_B\frac{\partial a}{\partial U_F}. \quad (16)$$

For a particular radius, variation in the inlet velocity, U_F, will cause variation in the area, a, by changing the angle of attack, α, and to a lesser extent by changing the local cavitation number, σ_L; thus

$$M_L = U_B\left[\frac{\partial a}{\partial\sigma_L}\frac{\partial\sigma_L}{\partial U_F} + \frac{\partial a}{\partial\alpha}\frac{\partial\alpha}{\partial U_F}\right]. \quad (17)$$

Because the inlet pressure is now held constant it follows that

$$\frac{\partial\sigma_L}{\partial U_F} = -\frac{\sigma_L U_F}{(U_F{}^2 + U_B{}^2)}; \quad \frac{\partial\alpha}{\partial U_F} = -\frac{\sin(\alpha+\beta)}{(U_F{}^2 + U_B{}^2)^{1/2}} \quad (18)$$

since $\cot(\alpha + \beta) = U_F/U_B$. Finally M_L becomes

$$M_L(\varphi, \sigma_T, r/R) = \sin(\alpha+\beta)\left[2\sigma_L\cos(\alpha+\beta)\frac{\partial a}{\partial\sigma_L} + \sin(\alpha+\beta)\frac{\partial a}{\partial\alpha}\right]. \quad (19)$$

Thus in order to evaluate the local mass flow gain factor and, by integration, the overall mass flow gain factor we need only evaluate the quantities $\partial a/\partial\alpha$ from the cascade analysis (in addition to the quantities $\partial a/\partial\sigma_L$ used in evaluating the compliance) It is worth anticipating the numerical results to note that the term in M_L involving $\partial a/\partial\sigma_L$ is generally much smaller than the $\partial a/\partial\alpha$ term. This is merely a reflection of the fact that $\sigma + \beta$ is generally close to $\pi/2$ so that

$$M_L \approx \frac{\partial a}{\partial\alpha}. \quad (20)$$

The parallel development of the compliance and mass flow gain factor permits us to write the following simple relation which is obtained by differentiation from equations (12), (20), (11), (15) and (4):

$$\left(\frac{\partial M_B}{\partial\sigma_T}\right)_{\varphi=\text{const}} \cong \left(\frac{\partial K_B}{\partial\varphi}\right)_{\sigma T=\text{const}}. \quad (21)$$

That is to say the rate of change of the mass flow gain factor with σ_T for constant φ must be approximately equal to the rate of change compliance with flow coefficient for constant σ_T. This relation can be most useful in interpreting the results for mass flow gain factor and compliance.

Some Examples

In order to present examples of compliances and mass flow gain factors the following turbopump inducer designs were selected:

A **Impeller III.** A simple inducer ($\beta_{r=R} = 81°$) whose blades

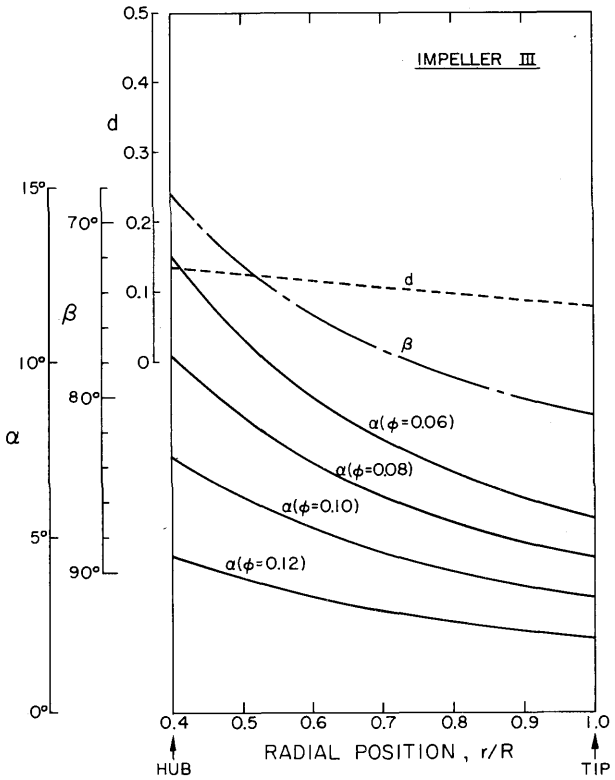

Fig. 3 Radial variations of the blade angle β, blade thickness to normal spacing ratio, d, and angle of attack, α, (for various flow coefficients, φ) for the simple helical inducer of Impeller III

lie along helical surfaces (similar to those employed in the cavitation studies of Acosta [28]). The hub ratio is 0.4 and the distributions of β, d and α (for various φ) are indicated in Fig. 3.

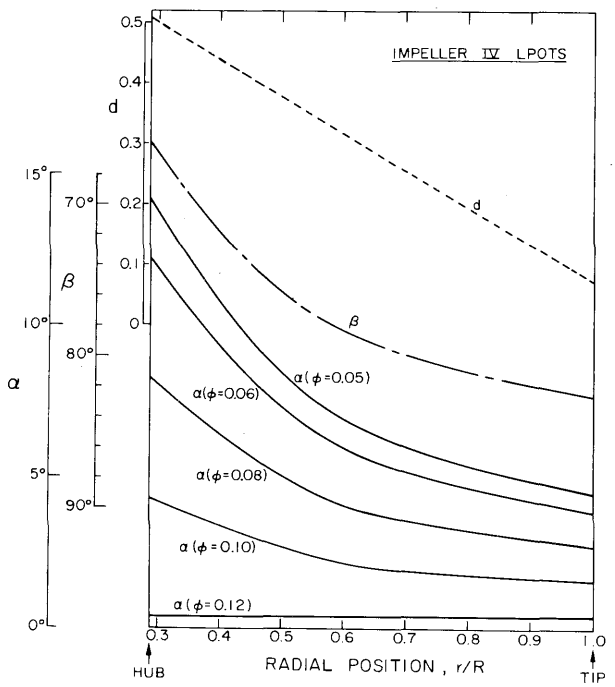

Fig. 4 Radial variations of the blade angle β, blade thickness to normal spacing ratio, d, and angle of attack, α, (for various flow coefficients, φ) for the low pressure oxidizer turbopump of the main shuttle engine (designated Impeller LPOTS).

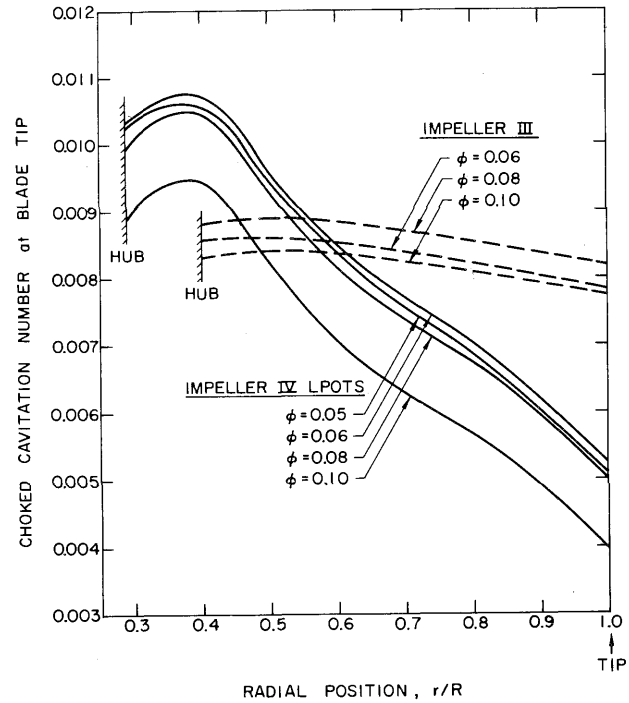

Fig. 5 The tip cavitation numbers at which the flow at each radial station becomes choked; values for both impellers and for various flow coefficients, φ

B **Impeller IV LPOTS.** This is the projected design for the inducer of the low pressure oxidizer pump to be used in the main engine of the Shuttle space vehicle. The radial distributions of β, d and α are indicated in Fig. 4. A primary reason for the choice of this impeller is the projection that this inducer will be important from the point of view of possible POGO instabilities. The high pressure oxidizer pump will also be important but will be less susceptible to cavitation; in the light of past experience, the fuel pumps are unlikely to be a major factor.

As described in detail by Brennen and Acosta [14] an important byproduct of the cascade analysis is the value of the tip cavitation number, σ_T, at which the flow at a particular radial station becomes choked. These values are shown in Fig. 5 and suggest that the breakdown cavitation number for the Impeller III will be close to 0.009 while that for the LPOTS inducer will be in the neighborhood of 0.011. The difference is primarily due to the fact that the blades of the LPOTS inducer are much thicker near the hub. Fig. 5 suggests choking will first occur near the hub of the LPOTS inducer as σ_T is reduced.

Examples of the radial distributions of compliance, K_L, and mass flow gain factor, M_L, are given in Figs. 6 and 7. From these we may anticipate that the overall mass flow gain factor will decrease much less rapidly than compliance as the cavitation number is raised. Integrated compliances, K_B, and mass flow gain factors, M_B, for the inducers are presented in Figs. 8 and 9.

Perhaps the most significant feature of these results is that, over most of the range of cavitation number, the mass flow gain factor, M_B, is very much larger than the compliance, K_B. This strongly suggests that any dynamic model for the transfer function, $[Z]$, which omits Z_{22} or M_B while retaining K_B could be significantly in error. In order to illustrate this it is necessary to delve more deeply into the models used by the dynamicists to extract compliance values from experimental observations.

Some Comparison With Test Observations of Saturn Engines

Since computed compliances, K_B, for the oxidizer (-0) and

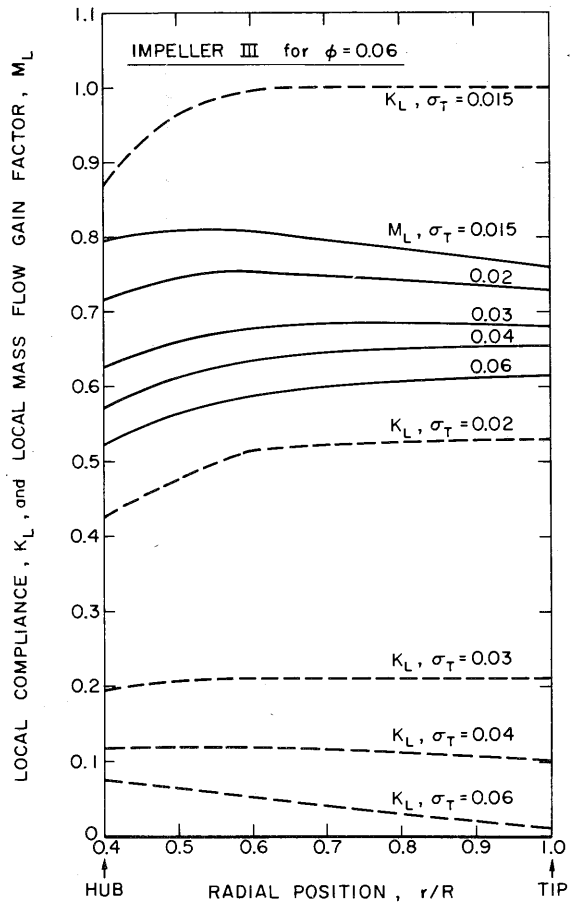

Fig. 6 Example of the radial distributions of compliance, K_L, and mass flow gain factor, M_L, for Impeller III at a flow coefficient of 0.06 and various tip cavitation numbers, σ_T

fuel ($-F$) turbopumps of the Saturn engines (J2, F1, H1) were compared with values deduced from experimental test observations (Vaage, Fidler and Zehnle [21]) in the earlier paper of Brennen and Acosta [14] it is appropriate that we should introduce calculated values of the mass flow gain factor into this picture and investigate whether the experimental observations can be explained in terms of this additional parameter. Since extensive tests were performed on the J2-0 turbopump, we select this for particular study. Fig. 10 presents the computed results for the compliance, K_B, and mass flow gain factor, M_B, of the J2-0 turbopump near the design flow coefficient ($\varphi = 0.097$) based on the radial distributions of blade angle and blade thickness included in Brennen and Acosta [14]. The circled points represent the values for the nondimensional compliance deduced from engine tests in the Rocketdyne facility (see below) and the difference between these experimental values (obtained by assuming $Z_{22} = 0$) and the theoretical K_B is clearly evident. This discrepancy would appear to be even greater for other Saturn turbopumps (Brennen and Acosta [14])

Lumped parameter electrical analogies have been employed to model the presumed dynamical behavior of rocket turbopumps; from these, experimental compliance values are deduced. The simplest model employed for example by Murphy (1969) visualizes the pump as consisting of a compliance element, C, a pressure (voltage) amplifier of gain, G, and a pump resistance, R_P as in Model A, Fig. 11. The discharge line is conventionally represented by an inertance, L, and a discharge resistance, R_D. However in the tests under consideration R_D was estimated to be small compared with R_P (Murphy [29] and private communication) so that for simplicity it is convenient to assume that it is absorbed in R_P and that the load merely consists of the inertance, L. In general the experimental observations which consist of pressure fluctuation measurements for inlet perturbations over a range of frequencies, Ω, are analyzed in the following way. First theoretical estimates are made for some of the quantities such as L, R_P and G, the last being close to unity (e.g.,

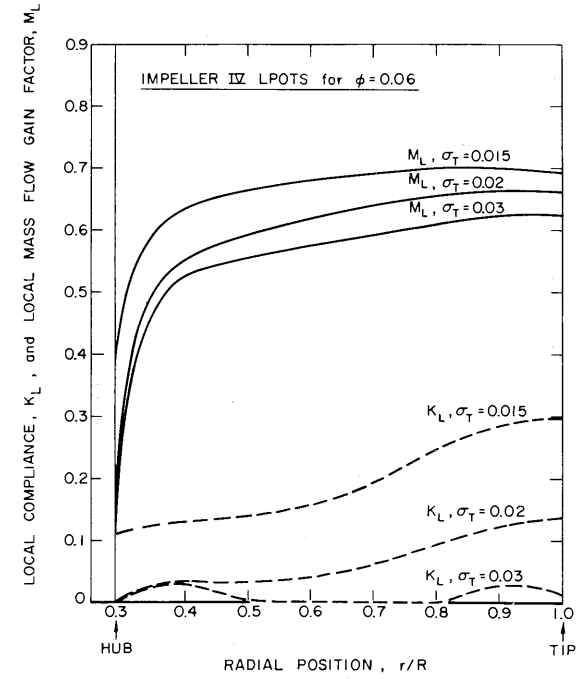

Fig. 7 Example of the radial distributions of compliance, K_L, and mass flow gain factor, M_L, for Impeller IV LPOTS at a flow coefficient of 0.06 and various tip cavitation numbers, σ_T.

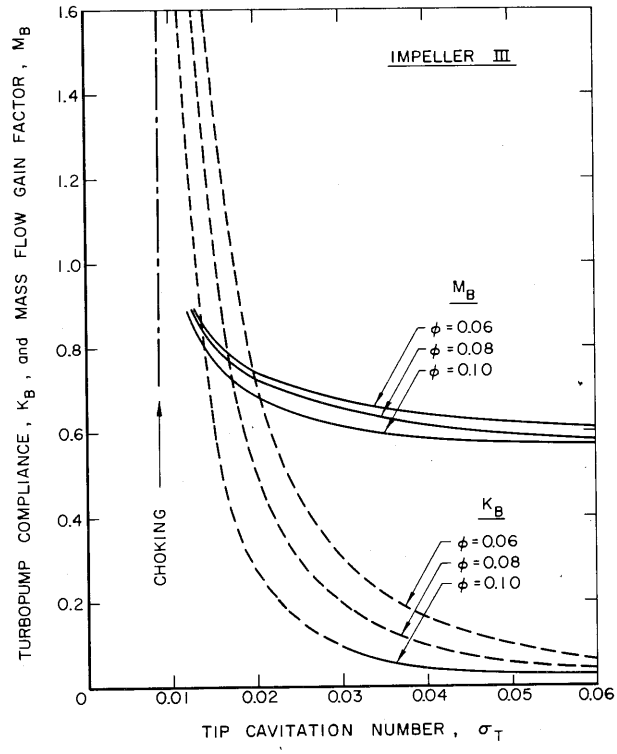

Fig. 8 Calculated compliance, K_B, and mass flow gain factor, M_B, for Impeller III as a function of flow coefficient, φ, and tip cavitation number, σ_T

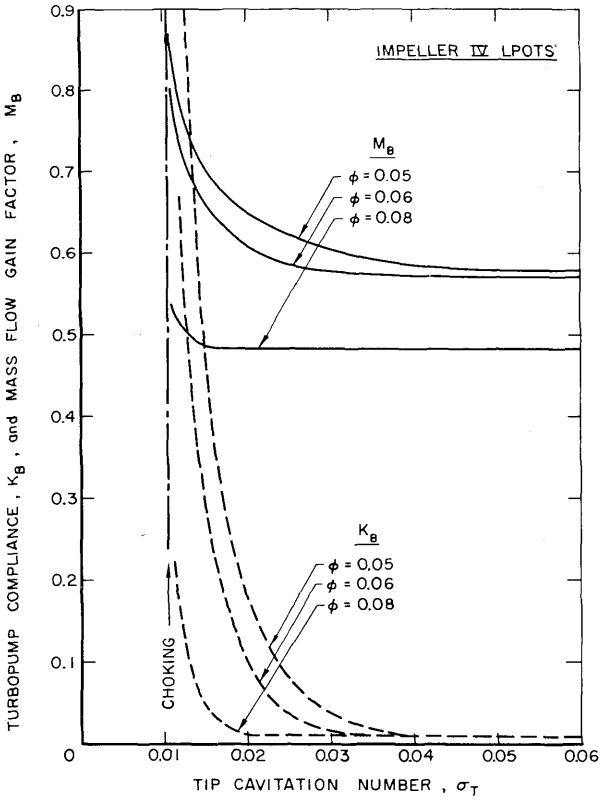

Fig. 9 Calculated compliance, K_B, and mass flow gain factor, M_B, for low pressure oxidizer turbopump in the main shuttle engine (Impeller IV LPOTS) as a function of flow coefficient and tip cavitation number, σ_T

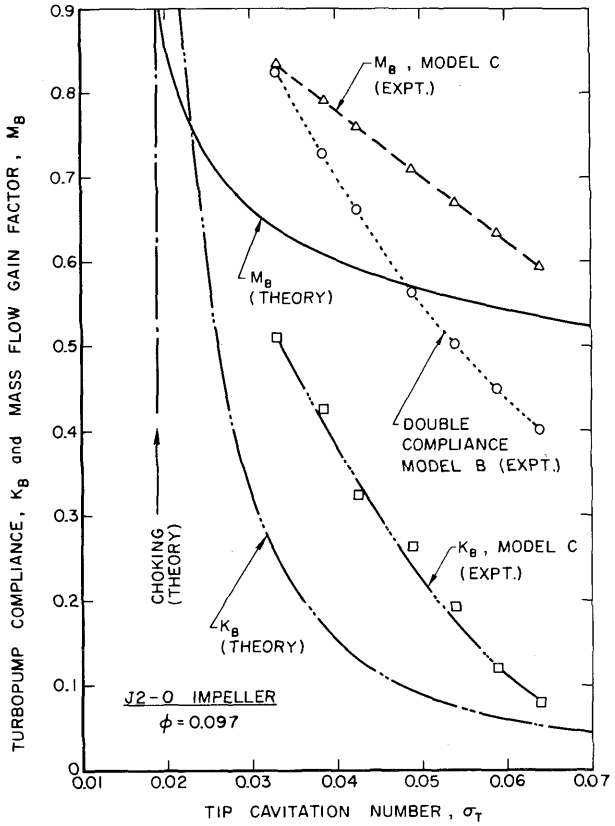

Fig. 10 Dynamic characteristics of the J2-0 turbopump. Theoretically calculated compliance, K_B, - - - - - - - -, and mass flow gain factor, M_B————, for φ = 0.097. Values derived from experimental observation: (1) main compliance, C, derived from double compliance Model B, O . . . . . O; (2) compliance, K_B, □ . . . . . □ and mass flow gain factor, M_B. Δ . . . . . Δ, from Model C of this paper

Murphy [29] used 1.2). Then the observations are analyzed to find the values of the compliance, C, at various cavitation numbers or suction pressures, which yield the best fit to the input impedance of the electrical analogy.

The most detailed investigation of this type was that performed on the J2-0 turbopump (references [21, 30, 31]). It was apparent from the results of those investigations that a single variable, C, was insufficient to properly match the observations. As a result a particular empirical model was proposed which seemed to fit the data quite well. This so-called "double compliance model" is shown as Model B in Fig. 11 and values for C, R_1/G, R_2/G, GC_2 and L/G are given by Vaage, Fidler and Zehnle [21]. Dimensional values for C and R_1/G are also listed in the first part of Table 1 and it is the nondimensional version of C which is plotted in Fig. 10. The input impedance of Model B is

$$\frac{\tilde{p}_1^*}{\tilde{m}_1^*} = \frac{R_1 + j\Omega(L + R_1R_2C_2) - \Omega^2LC_2R_2}{G + j\Omega(CR_1 + GC_2R_2) - \Omega^2(LC + R_1CR_2C_2) - j\Omega^3LCR_2C_2}. \quad (22)$$

Now consider Model C which we might construct from the considerations of this paper. It consists of a pump transfer function containing a gain, G, a pump resistance, R_P, the dimensional mass flow gain factor, M_B^*, and the dimensional compliance, C_B. The input impedance is thus

$$\frac{\tilde{p}_1^*}{\tilde{m}_1^*} = \frac{R_P + j\Omega(L - M_B^*R_P) + \Omega^2M_B^*L}{G + j\Omega C_BR_P - \Omega^2LC_B}. \quad (23)$$

Now in comparing (22) and (23) it is well to remember the limitations of our quasistatic analysis and therefore the transfer function. The analysis cannot predict variations in M_B^* and C_B when ω is no longer small. Therefore if the expressions (22) and (23)

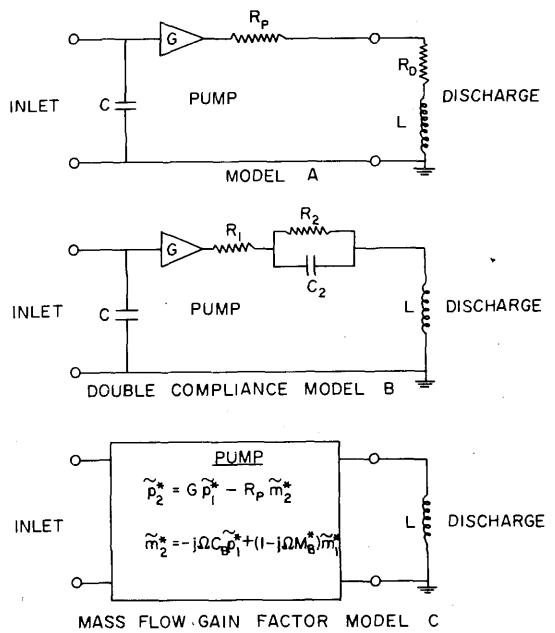

Fig. 11 Electronic analogies for the dynamic behavior of cavitating turbopumps and the mass flow gain factor Model C of this paper

are equated and the result arranged as a polynomial in $j\Omega$ we are only justified in equating the coefficients of first two terms in the polynominal, at most. The first coefficient obviously yields $R_P = R_1$; the second coefficient gives

$$C - C_B = \frac{M_B{}^* G}{R_1} \quad (24)$$

Thus dynamic behavior equivalent to that of the Double Compliance Model can be constructed from a mass flow gain factor, $M_B{}^*$, and a compliance, C_B, which are related through equation (24) to the values for C and R_1/G given in Table 1. This simple analysis cannot separate C_B and $M_B{}^*$ but a set of dimensional values consistent with the experimental data [30, 31 and 21] are listed in Table 1 and plotted nondimensionally in Fig. 10. Comparing these with the theoretical values of K_B and M_B it is clear that there is significantly better agreement than between the Double Compliance Model compliance alone and the theoretical K_B. Indeed, given the approximate nature of the experimental data the agreement is most encouraging. Furthermore, it should be noted that the somewhat greater experimental compliance and mass flow gain factor could arise through contributions from tip vortex, backflow and bubble cavitation volumes which are not, of course, included in the present theory.

Table 1 Numerical values for the J2-0 turbopump according to the Model B, Fig. 10 from Vaage, Fidler and Zehnle [21] and equivalent values of C_B and $M_B{}^*$ for the mass flow gain factor Model C

Tip cavitation number	Double compliance Model B		Mass flow gain[a] factor model C	
	C ($m^2 \times 10^5$)	R_1/G ($m^{-2}s \times 10^{-3}$)	C_B ($m^2 \times 10^5$)	$M_B{}^*$ ($s \times 10^2$)
0.0330	1.22	0.65	0.76	0.30
0.0385	1.13	0.57	0.64	0.28
0.0425	0.91	0.58	0.48	0.27
0.0490	0.86	0.54	0.41	0.25
0.0540	0.79	0.49	0.30	0.24
0.0590	0.66	0.47	0.17	0.23
0.0635	0.52	0.51	0.11	0.21

[a]For the J2-0 pump the nondimensional K_B is given by $C_B/(1.48 \times 10^{-5}\ m^2)$ and the nondimensional M_B by $M_B{}^* \times (279 s^{-1})$

Concluding Remarks

It has been demonstrated that a transfer function which includes not only a compliance element but also a mass flow gain factor is a satisfactory first approximation for a cavitating pump. In the past, neglect of this latter factor led to large discrepancies between compliances estimated theoretically on the basis of free streamline solutions of the fully cavitating cascade flow through an inducer and "compliances" evaluated from experimental observation of the dynamic behavior of cavitating pumps. When the latter are analyzed with prior knowledge of the existence of a mass flow gain factor when the differences between the theory and experimental observations are very much smaller and the comparison provides support for the validity of the theoretical model. The experimental values of compliance and mass flow gain factor still appear to be somewhat higher than the theoretical values. Since the theory of the present paper considers only fully developed blade cavities and neglects the volume of tip vortex, backflow and bubble cavities it would seem reasonable to associate this latter volume with the remaining discrepancy.

However there are also limitations to the present theory which require attention. In the first place it is limited to low reduced frequencies. Furthermore we have thus far evaluated only the first term in each of the elements of the transfer function. In this respect it would appear that the next important step would be to determine the first order frequency dependence of the pump gain Z_{11} (or G) and the pump resistance Z_{12} (or R_P); indeed there are experimental indications of significant differences between static and dynamic pump gains [15]. Such effects would have to be included in Model C, Fig. 11 and would influence the values of compliance and mass flow gain factor derived from the experimental observations.

Clearly, however, there is a dire need for more specific and detailed experimental data on the complete transfer function. Such experiments, unlike the previous tests, should measure directly the fluctuating pressures *and* mass flow rates at inlet and discharge and thus permit conclusive comparison between theory and experiment. We are presently involved in such an experiment and hope to present such results in the near future.

Acknowledgment

The authors are indebted to the George Marshall Space Flight Center, Huntsville, Alabama for support under NASA Contract NAS 8-28046 and to Mr. L. Gross of NASA, Huntsville, Dr. S. Rubin of Aerospace Corporation and Dr. J. Fenwick of the Rocketdyne Division of Rockwell International for valuable suggestions and advice.

References

1 Jaeger, C., "The Theory of Resonance in Hydro-Power Systems, Discussion of Incidents and Accidents Occurring in Pressure Systems," *Journal of Basic Engineering*, Vol. 85, 1963, pp. 631–640.

2 Streeter, V. L., and Wylie, E. B., "Waterhammer and Surge Control," *Annual Review of Fluid Mechanics*, Vol. 6, 1974, pp. 57–73.

3 Liao, G. S., "Protection of Boiler Feed Pump Against Transient Suction Decay," *Journal of Engineering for Power*, Vol. 96, 1974, pp. 247–255.

4 Liao, G. S., and Leung, P., "Analysis of Feedwater Pump Suction Pressure Decay Under Instant Turbine Load Rejection," *Journal of Engineering for Power*, Vol. 34, 1972, pfi. 83–90.

5 Zielke, W., and Hack, H. P., "Resonance Frequencies and Associated Mode Shapes of Pressurized Piping Systems," *International Conference Pressure Surges*, Paper G-1, Brit. Hydromech. Res. Assoc., Cranfield, England, G1-1-13, 1972.

6 Wijngaarden, L. van, "On the Equations of Motion for Mixtures of Liquid and Gas Bubbles," *Journal of Fluid Mechanics*, Vol. 33, 1968, p. 465.

7 Weyler, M. E., Streeter, V. L., and Larsen, P. S., "An Investigation of the Effect of Cavitation Bubbles on the Momentum Loss in Transient Pipe Flow," *Journal of Fluids Engineering*, Vol. 93, 1971, pp. 1–10.

8 Safwat, H. H., and Van Den Polder, J., "Experimental and Analytical Data Correlation Study of Water Column Separation," *Journal of Fluids Engineering*, TRANS. ASME, Vol. 95, 1973, pp. 91–97.

9 Knapp, R. T., "Complete Characteristics of Centrifugal Pumps and Their Use in the Prediction of Transient Behavior," TRANS. ASME, Nov. 1937, pp. 683–689.

10 Prevention of coupled-structure propulsion instability (POGO), NASA SP-8055, Oct. 1970.

11 Rubin, S., "Longitudinal Instability of Liquid Rockets due to Propulsion Feedback (POGO)," *Journal of Spacecraft and Rockets*, Vol. 3, No. 8, 1966, pp. 1188–1195.

12 Sack, L. E., and Nottage, H. B., "System Oscillations Associated With Cavitating Inducers," *Journal of Basic Engineering*, Vol. 87, Series D, No. 4, 1965, pp. 917–925.

13 Natanzon, M. S., Bal'tsev, N. I., Bazhanov, V. V., and Leydervarger, M. R., "Experimental Investigations of Cavitation-Induced Oscillations of Helical Inducers," *Fluid Mechanics Soviet Research*, Vol. 3, 1974, pp. 38–45.

14 Brennen, C., and Acosta, A. J., "Theoretical, Quasi-Static Analysis of Cavitation Compliance in Turbopumps," *Journal of Spacecraft and Rockets*, Vol. 10, No. 3, 1973, pp. 175–180.

15 Wagner, R. G., "Titan II Engine Transfer Function Test Results," Report No. TOR-0059 (6471)-9, Aerospace Corporation, El Segundo, Calif., Feb. 1971.

16 Kim, J. H., and Acosta, A. J., "Unsteady Flow in Cavitating Turbopumps," *Journal of Fluids Engineering*, Vol. 96, 1974, pp. 25–28.

17 Furuya, O., "Unsteady Cavitating Cascade Flow," unpublished report, 1975.

18 Rubin, S., Wagner, R. G., and Payne, J. G., "Pogo Suppression on Space Shuttle—Early Studies," NASA Report CR-

2210, Mar. 1973.
19 Ghahremani, F. G., and Rubin, S., "Empirical Evaluation of Pump Inlet Compliance," Final Report No. ATR-73 (7257)-i, Aerospace Corporation, El Segundo, Calif., July 1972.
20 Brennen, C., "The Dynamic Behavior and Compliance of a Stream of Cavitating Bubbles," *Journal of Fluids Engineering*, Vol. 95, Series 1, No. 4, 1974, pp. 533–542.
21 Vaage, R. D., Fidler, L. E., and Zehnle, R. A., "Investigation of Characteristics of Feed System Instabilities," Final Report MCR-72-107, Martin Marietta Corporation, Denver, Colo., May 1972.
22 Cohen, H., and Sutherland, C. D., "Finite Cavity Cascade Flow," *Math. Rep. 14*, Apr. 1958, Rensselaer Polytechnic Inst., Troy, N.Y.
23 Acosta, A. J., and Hollander, A., "Remarks on Cavitation in Turbomachines," Rept. E-79.3, Oct. 1959, Eng. Science Dept., Calif. Inst. of Tech., Pasadena, Calif.
24 Acosta, A. J., "Cavitating Flow Past a Cascade of Circular Arc Hydrofoils," Rept. E-79.2, Eng. Science Dept., Calif. Institute of Technology, Pasadena, Calif., Mar. 1960.
25 Wade, R. B., "Linearized Theory of a Partially Cavitating Cascade of Flat Plate Hydrofoils," *Applied Science Research*, Vol. 17, No. 3, 1967, pp. 169–188.
26 Stripling, L. B., and Acosta, A. J., "Cavitation in Turbopumps—Part I," *Journal of Basic Engineering*, Vol. 84, No. 3, Sept. 1962, pp. 326–338.
27 Lakshminarayana, B., "Three-Dimensional Flow Field in Rocket Pump Inducers. Part I: Measured Flow Field Inside the Rotating Blade Passage and at the Exit," *Journal of Fluids Engineering*, Vol. 95, 1973, pp. 567–578.
28 Acosta, A. J., "An Experimental Study of Cavitating Inducers," *Proceedings of Second O.N.R. Symposium on Naval Hydrodynamics*, August 25–29, 1958, ACR-38.
29 Murphy, G. L., "Pogo Suppression Analysis of the S-II and S-IVB LOX Feed Systems," Summary Report ASD-ASTN-1040, Brown Engineering Co., Huntsville, Ala., 1969.
30 Rocketdyne Report, "J-2 Vehicle Longitudinal Stability (POGO) Analysis Program," Rocketdyne Division, North American Rockwell, Report No. R-6283, Aug. 1965.
31 Rocketdyne Report, "Investigation of 17-Hz, closed-loop instability on S-II Stage of Saturn V," Rocketdyne Division, North American Rockwell, Report No. R-7970, Aug. 1969.
32 Kolesnikov, K. S., and Kinelev, V. G., "Mathematical Model of Cavitation Phenomena in Heilocentrifugal Pumps," *Soviet Aeronautics*, Vol. 16, No. 4, 1973, pp. 64–68.

APPENDIX I

Variation of the Rotational Velocity

By way of further information it is useful to evaluate the additional effects which occur when the rotational speed fluctuates in response to the fluctuating loading or due to some other dynamic linkage between the fluid flow and the impeller drive system, such as a turbine drive requiring a bleed from the through flow. The matrix Z must then be expanded to

$$\begin{Bmatrix} \tilde{p}_2 - \tilde{p}_1 \\ \tilde{m}_2 - \tilde{m}_1 \end{Bmatrix} = \begin{bmatrix} Z_{11} & Z_{12} & Z_{13} \\ Z_{21} & Z_{22} & Z_{23} \end{bmatrix} \begin{Bmatrix} \tilde{p}_1 \\ \tilde{m}_1 \\ \tilde{N} \end{Bmatrix} \quad (25)$$

where $\tilde{N}$ describes the phase and amplitude of the fluctuating rotational speed, nondimensionalized with respect to the mean rotational speed. As with Z_{11} and Z_{12} the quasistatic value of Z_{13} may be obtained from the steady state pump characteristic which describes the variation of pressure rise with rotational speed when both the suction pressure and inlet mass flow remain constant. Thus we concentrate here on Z_{23} which is given by

$$Z_{23} = \left(\frac{\tilde{m}_2 - \tilde{m}_1}{\tilde{N}} \right)_{\tilde{p}_1 - \tilde{m}_1 = 0} = j \frac{\Omega}{A_i} \left(\frac{\partial V}{\partial U_T} \right)_{\tilde{p}_1 - \tilde{m}_1 = 0}. \quad (26)$$

In a manner analogous with the compliance and the mass flow gain factor we define a quantity called the rotational influence factor, N_B, so that

$$Z_{23} = -j\omega N_B \quad (27)$$

Further we define local rotational influence factors, N_L, such that

$$N_B = \frac{2}{[1 - (R_H/R)^2]} \int_{R_H/R}^{1} N_L(\varphi, \sigma_T, r/R) d\left(\frac{r}{R}\right) \quad (28)$$

where it follows from equations (26), (27), (28) and the definitions of previous sections that

$$N_L = -\frac{U_B r^2}{R^2} \left[\frac{\partial a}{\partial \alpha} \frac{\partial \alpha}{\partial U_B} + \frac{\partial a}{\partial \sigma_L} \frac{\partial \sigma_L}{\partial U_B} \right]$$

$$= \sin(\alpha + \beta) \frac{r^2}{R^2} \left[2\sigma_L \sin(\alpha + \beta) \frac{\partial a}{\partial \sigma_L} - \cos(\alpha + \beta) \frac{\partial a}{\partial \alpha} \right]. \quad (29)$$

Thus with the derivatives $\partial a/\partial \sigma_L$ and $\partial a/\partial \alpha$ which have already been calculated from the cascade analysis for the evaluation of compliance and mass flow gain factor we may also evaluate the local rotational influence factors, N_L, and thus, by integration, the overall factor, N_B. But as previously mentioned $(\alpha + \beta)$ is generally close to $\pi/2$; hence N_L is approximately given by

$$N_L \approx 2 \frac{r^2 \sigma_L}{R^2} \frac{\partial a}{\partial \sigma_L} \cong 2\sigma_T \frac{\partial a}{\partial \sigma_L} = -2\sigma_T K_L. \quad (30)$$

Hence after integration it follows that

$$N_B \approx -2\sigma_T K_B. \quad (31)$$

This simple relation between the rotational influence factor and the dimensionless compliance of the pump is of considerable value in assessing the importance of the role played by fluctuations in the rotational speed. By substitution of equation (31) into the transfer matrix it is readily observed that the relative or fractional speed variation, $\tilde{N}$, has a negligible effect on the transfer function only when

$$\tilde{N} << \tilde{p}_1^*/\rho U_T^2 \sigma_T. \quad (32)$$

Conversely the speed variation dominates the inlet pressure fluctuation entirely when $\tilde{N} >> \tilde{p}_1^*/\rho U_T^2 \sigma_T$. Comparison of these quantities merely amounts to comparison of the percentage fluctuations in rotational speed and cavitation number.